

See discussions, stats, and author profiles for this publication at: <https://www.researchgate.net/publication/30767854>

High H₂ Storage of Hexagonal Metal–Organic Frameworks from First–Principles–Based Grand Canonical Monte Carlo Simulations

ARTICLE *in* THE JOURNAL OF PHYSICAL CHEMISTRY C · SEPTEMBER 2008

Impact Factor: 4.77 · DOI: 10.1021/jp800832b · Source: OAI

CITATIONS

51

READS

20

4 AUTHORS, INCLUDING:



Sang Soo Han

Korea Research Institute of Standards and ...

58 PUBLICATIONS 1,900 CITATIONS

SEE PROFILE



William A. Goddard

California Institute of Technology

1,347 PUBLICATIONS 69,067 CITATIONS

SEE PROFILE

High H₂ Storage of Hexagonal Metal–Organic Frameworks from First-Principles-Based Grand Canonical Monte Carlo Simulations

Sang Soo Han and William A. Goddard III*

Materials and Process Simulation Center (MC 139-74), California Institute of Technology, Pasadena, California 91125

Received: January 28, 2008; Revised Manuscript Received: May 1, 2008

Stimulated by the recent report by Yaghi and co-workers of hexagonal metal–organic frameworks (MOF) exhibiting reversible binding of up to 7.5 wt % at 77 K and 70 bar for MOF-177 (called here IRMOF-2-24), we have predicted additional trigonal organic linkers, including IRMOF-2-60, which we calculate to bind 9.7 wt % H₂ storage at 77 K and 70 bar, the highest known value for 77 K. These calculations are based on grand canonical Monte Carlo (GCMC) simulations using force fields that match accurate quantum mechanical calculations on the binding of H₂ to prototypical systems. These calculations were validated by comparison to the experimental loading curve for IRMOF-2-24 at 77 K. We then used the theory to predict the effect of doping Li into the hexagonal MOFs, which leads to substantial H₂ density even at ambient temperatures. For example, IRMOF-2-96-Li leads to 6.0 wt % H₂ storage at 273 K and 100 bar, the first material to attain the 2010 DOE target.

1. Introduction

A major technical obstacle to the widespread use of hydrogen as a nonpolluting fuel for automobiles is the lack of a safe and efficient system for on-board storage. Recently Yaghi and co-workers pioneered the metal–organic frameworks (MOFs), a new class of ordered, three-dimensional extended solids composed of metal ions and organic linkers that comprise promising material for H₂ storage.¹ For example cubic crystalline MOF-5 (denoted herein as IRMOF-1-6) has an extraordinarily low density (0.59 g/cc) and high surface area (3534 m²/g) while binding 5.2 wt % of H₂ at 77 K and 45 bar.² These cubic crystalline MOFs show increasing H₂ density as the size of the aromatic organic linker increases, particularly with increased pressure.^{3,4} Indeed we recently reported⁴ that cubic crystalline MOF-C30 (denoted herein as IRMOF-1-30) exhibits H₂ storage of 6.5 wt % at 77 K and 20 bar, and that using Mg based nodes increases the hydrogen storage capacity up to 8.1 wt % for 20 bar.

Recently the Yaghi group reported that hexagonal MOF-177 (denoted herein as IRMOF-2-24) shows a H₂ uptake of 7.5 wt % at 77 K and 70 bar, the highest experimental value reported to date.² Even so these best current MOF materials do not meet the 2010 DOE (Department of Energy) criteria for use in transportation (at least 6.0 wt % for temperatures above 243 K at pressures below 100 bar).⁵ We recently predicted that doping these cubic MOFs with lithium, Li can lead to an uptake of 6.0 wt % at 243 K and 100 bar.⁶

In this work, we report the H₂ adsorption behavior for hexagonal MOFs with a variety of organic linkers. We find new hexagonal MOFs that show increased H₂ uptake compared to cubic. For example, the IRMOF-2-60 has a H₂ storage capacity of 9.7 wt % at 77 K and 90 bar, higher than the best previous report for undoped MOFs (7.5 wt % for MOF-177).²

In addition, we find that lithium doping enhances H₂ storage of the hexagonal MOFs at ambient temperature. Thus, Li-doped

IRMOF-2-96 is predicted to have a remarkable H₂ storage capacity of 6.5 wt % at 243 K and 100 bar, and meets the 2010 DOE target of 6.0 wt % even at 273 K and 100 bar.

2. Notation

As Omar Yaghi pioneered the isorecticular MOF systems, the numbering scheme was more-or-less chronological, e.g., MOF-1, MOF-2, etc. As other workers entered the field, they generally worked together with Prof. Yaghi to assign unique names ever for materials that Yaghi had not developed. In our work on cubic MOF materials, we used a simpler naming convention that included the number of carbons in the organic linkers and added notations when other metals were used in the inorganic linkers or when dopants such as Li were added.^{4,6} Thus

- MOF-5 (IRMOF-1) of Yaghi was MOF-C6 in Han and Goddard (HG).
- MOF-8 of Yaghi was MOF-C10 in HG.
- MOF-C30 of HG was a new compound not previously synthesized experimentally.

In order to systematize the naming to make it more mnemonic, we have agreed with Prof. Yaghi to a modified notation that we can both use for future papers. We plan a joint paper to discuss this notation, but the current paper has been switched to the new notation.

The general form for the MOF materials is

- an inorganic node with n points each connected to an organic ligand and
- organic linker ligands with m connecting points each connected to an inorganic node.

Thus the cubic MOFs (e.g., MOF-5 and IRMOF-8) have $n = 6$ and $m = 2$ or {6,2}. On the other hand the hexagonal MOF (MOF-177) has $n = 6$ and $m = 3$ or {6,3}.

We will now refer to

- all MOFs with the {6,2} topology as the isorecticular MOF-1 family or IRMOF-1.
 - All MOFs with the {6,3} topology the IRMOF-2 family.
- Within each family, we use a name referring to the number of carbons in the linker. In this notation

* To whom correspondence should be addressed. E-mail: wag@wag.caltech.edu.

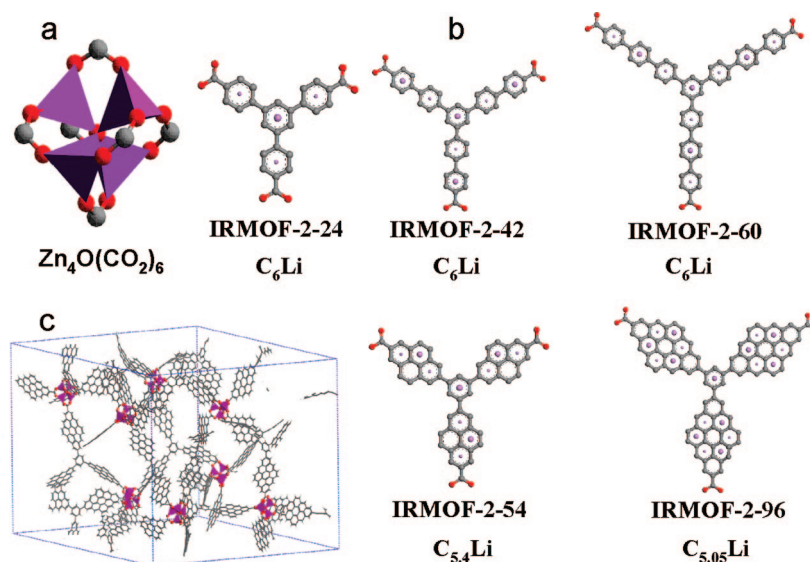


Figure 1. Atomistic structures of hexagonal MOFs. The $\text{Zn}_4\text{O}(\text{CO}_2)_6$ connector (a) couples to six organic linkers (b) through the O–C–O common to each linker. The large violet atoms in the linkers represent Li atoms above the linkers while small violet Li atoms lie below the linker. An overview of the IRMOF-2-96 crystal structure is shown in (c). IRMOF-2-24 was previously synthesized experimentally by Yaghi and co-workers (denoted as MOF-177).

TABLE 1: Physical Properties of Hexagonal MOFs

property	IRMOF-2-24 ^b	IRMOF-2-42	IRMOF-2-60	IRMOF-2-54	IRMOF-2-96
lattice parameter ^a (Å)	a: 37.3227 ^b c: 30.1416 ^b	a: 47.8560 c: 39.9479	a: 61.3717 c: 50.6624	a: 47.4396 c: 38.9639	a: 60.6735 c: 51.8335
surface area ^c (m ² /g)	4780 ^d (4834) ^e	5722 ^d (5718) ^e	6331 ^d (6316) ^e	5112 ^d (5116) ^e	5175 ^d (5278) ^e
free volume ^d (cm ³ /g)	1.54 ^d (1.38) ^e	2.82 ^d (2.55) ^e	5.08 ^d (4.63) ^e	2.17 ^d (1.88) ^e	3.39 ^d (2.94) ^e

^a Optimized structures using the DREIDING force field.⁸ All hexagonal MOFs have crystals with $\alpha = \beta = 90^\circ$, $\gamma = 120^\circ$. ^b This material was denoted as MOF-177. Experimental values are $a = 37.0720$ and $c = 30.0333$ at 300 K. ^c Solvent accessible surface area calculated assuming a probe radius of 1.2 Å (using Cerius2). ^d For pure MOFs. ^e For Li doped MOFs. ^f Solvent accessible free volume assuming a probe radius of 1.2 Å (using Cerius2).

- MOF-5 of Yaghi which is the MOF-C6 of HG becomes IRMOF-1-6.
- MOF-8 of Yaghi which is the MOF-C10 of HG becomes IRMOF-1-10.
- MOF-C30 of HG becomes IRMOF-1-30.
- MOF-177 of Yaghi becomes IRMOF-2-24.

For Li doped MOF materials, e.g. the best for H_2 storage, which was previously denoted as Li-MOF-C30, we now use the notation IRMOF-1-30-Li.

In this paper, we will consider generalizations of the MOF-177 hexagonal family (i.e., IRMOF-2-24) to five other hexagonal systems.

3. Computational Details

Our previous studies⁴ showed that the maximum H_2 storage for MOFs depends on the organic linker. Thus in this work we considered H_2 uptake behavior of hexagonal MOFs with a variation of organic linkers.

Figure 1 shows the atomistic structures of several MOFs considered in this work. Here we use the $\text{Zn}_4\text{O}(\text{CO}_2)_6$ cluster as the node to link trigonal organic aromatics to form hexagonal structures. In these systems the interactions of the central aryl unit causes a 33 to 71° twist of the three attached aromatic units, leading to C_3 symmetry. For the Li doped systems, we determined the positions of Li atoms using density functional theory (X3LYP flavor),⁷ finding that the Li atoms on adjacent aromatic rings are on opposite sides.⁶ Moreover various physical

properties (lattice parameters, surface area and free volume) of hexagonal MOFs considered in this study are summarized in Table 1.

To calculate the H_2 uptake of hexagonal MOFs as a function of temperature and pressure, we used the grand canonical ensemble Monte Carlo (GCMC) technique.⁹ To obtain an accurate measure of H_2 loading, we constructed 10 000 000 configurations to compute the average loading for each temperature and pressure. This determines the equilibrium loading of H_2 as a function of pressures and temperature. To eliminate boundary effects, we used an infinite three dimensionally periodic cell containing 32 Zn atoms.

The force field used in the GCMC calculations was based on quantum mechanics (QM) [second order Møller-Plesset (MP2)] expected to yield accurate binding energies of H_2 to the MOF materials. For binding H_2 to the metal-oxide cluster the MP2 used the triple- ζ TZVPP basis sets, while for binding H_2 to the organic linkers, we used MP2 with the quadruple- ζ QZVPP basis set. Similar calculations were used to describe the interaction of H_2 with aromatics doped with Li.^{4,5}

These methods were validated by comparing to the experimental H_2 density of cubic MOF systems (IRMOF-1-6), where we found 1.28 wt % at 77 K and 1 bar compared to 1.32 wt % experimental.⁴ We report here additional validations for the hexagonal systems.

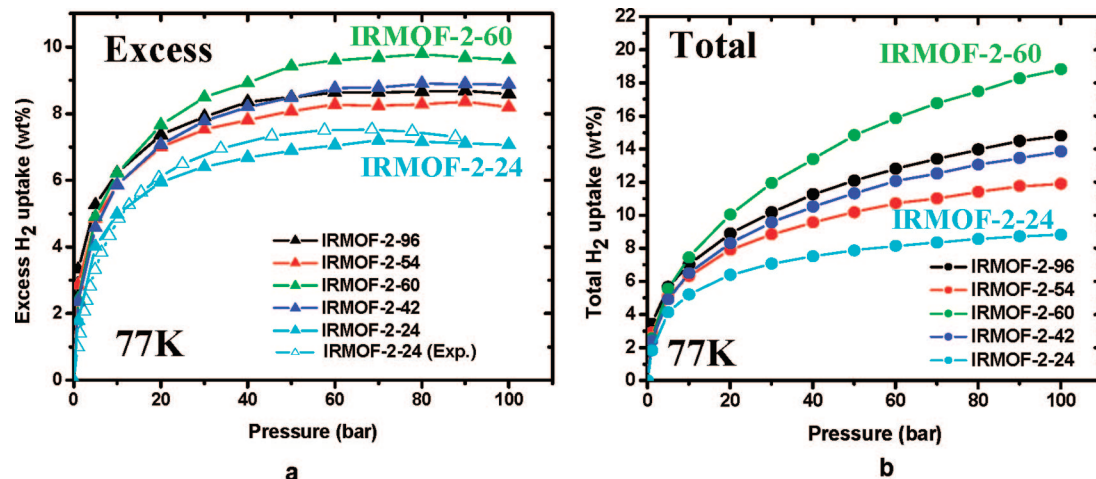


Figure 2. Predicted excess H₂ (a) and total H₂ (b) isotherms for hexagonal MOF systems at 77 K. The experimental data on IRMOF-2-24 (known previously as MOF-177) is from ref 2. Here the color code is cyan = IRMOF-2-24, blue = IRMOF-2-42, green = IRMOF-2-60, red = IRMOF-2-54, and black = IRMOF-2-96.

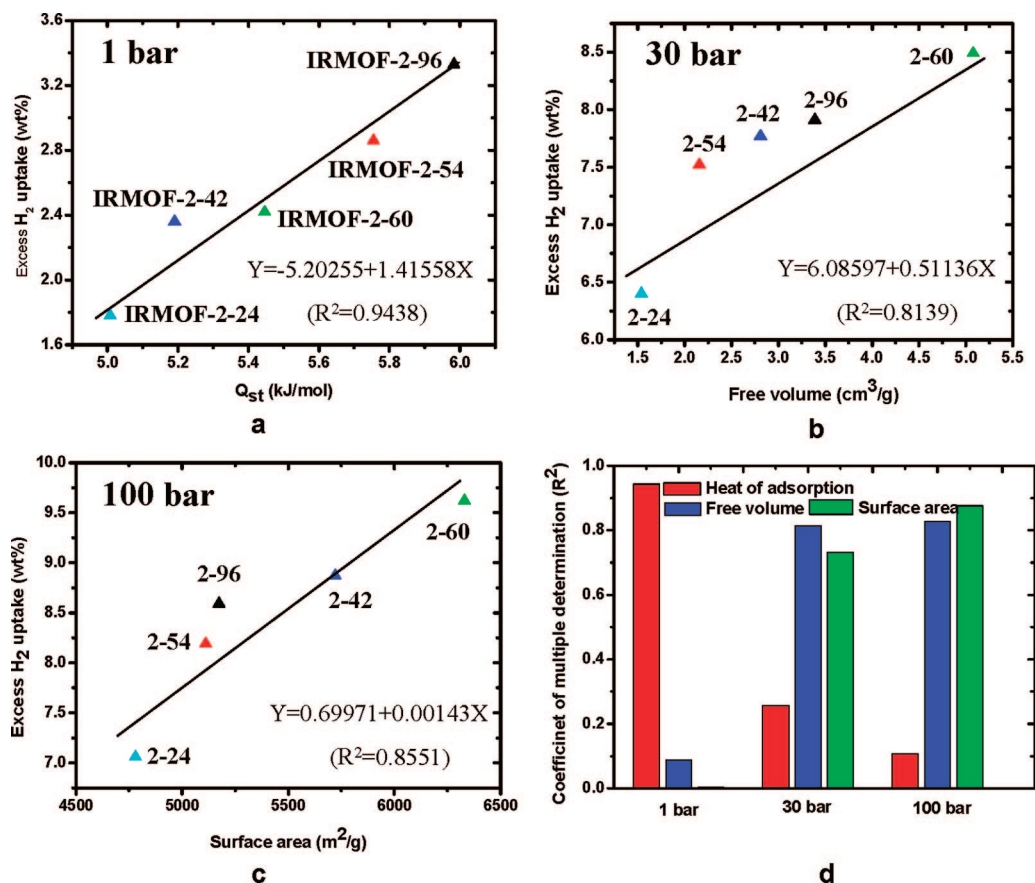


Figure 3. Effects of isosteric heat of adsorption (Q_{st}) (a), free volume (b), and surface area (c) of MOFs on excess H₂ uptake in pure MOFs at 1 (a), 30 (b), and 100 bar. A linear regression analysis of this data leads to the contributions shown in (d) where an R^2 near 1 indicates a good correlation.

4. Results and Discussion for Pure New Hexagonal MOF Materials

4.1. H₂ Storage at 77 K. Figure 2 shows the excess H₂ isotherm and total H₂ isotherm of pure hexagonal MOFs at 77 K up to 100 bar. The excess H₂ storage was calculated as the total amount of H₂ gas contained in the pores minus the amount of the gas that would be present in the pores in the absence of gas–solid intermolecular forces.¹⁰ For IRMOF-2-24 (known previously as MOF-177), our simulated H₂ isotherm is in good agreement with experiment.² For example we calculate 7.1

wt % at 80 bar which can be compared to 7.4 wt % from experiment at 70 bar.²

Our simulations find the highest H₂ density for IRMOF-2-60: 9.7 wt % at 90 bar. It is higher than the maximum capacity of 7.2 wt % for the best cubic MOF⁴ using Zn₄O(CO₂)₆ inorganic linkers, IRMOF-2-60 (known previously as MOR-C30).

None of the total H₂ uptake isotherms are saturated at 100 bar. The total H₂ storage capacities at 100 bar are 8.8 wt % for IRMOF-2-24, 11.9 wt % for IRMOF-2-54, 13.9 wt % for

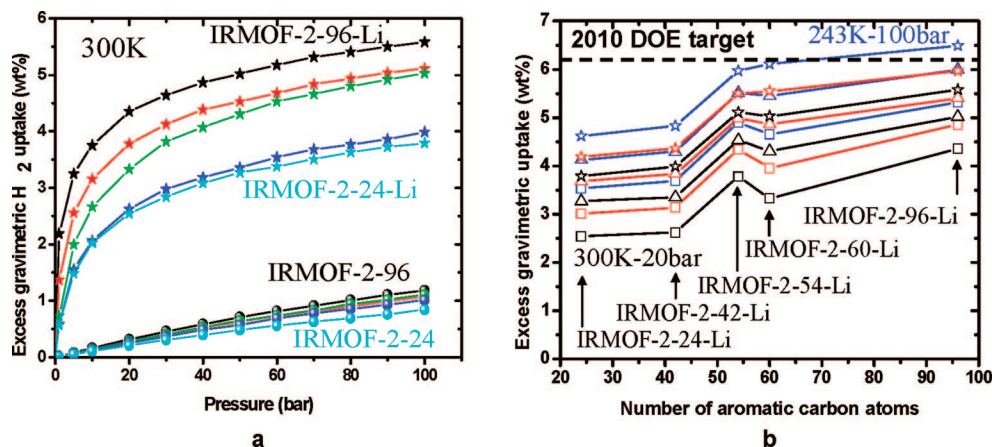


Figure 4. Predicted excess H₂ adsorption isotherms in gravimetric units (wt %) at 300 K for pure MOFs (circles) and Li doped MOFs (stars). Here the color code is IRMOF-2-24-Li = cyan, IRMOF-2-42-Li = blue, IRMOF-2-60-Li = green, IRMOF-2-54-Li = red, and IRMOF-2-96-Li = black. (a) predicted excess H₂ storage for IRMOF-2-xx-Li (xx = 24, 42, 54, 60, and 96) as a function of temperature and pressure. And (b) predicted excess H₂ storage for IRMOF-2-xx-Li (xx = 24, 42, 54, 60, and 96) at various temperatures for 100 bar as a function of linker carbons. The DOE target of 6 wt % is achieved for IRMOF-2-96-Li. Here the symbol code is 243 K = star, 273 K = triangle, and 300 K = square and black = 20 bar, red = 50 bar, and blue = 100 bar.

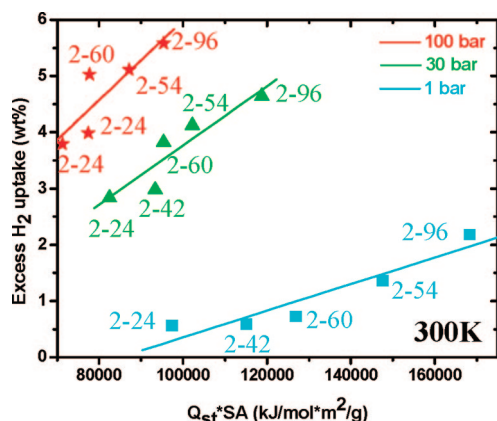


Figure 5. Relationship between H₂ uptake in IRMOF-Li at 300 K and multiple values of heat of adsorption (Q_{st}) and surface area (SA).

IRMOF-2-42, 14.8 wt % for IRMOF-2-96, and 18.8 wt % for IRMOF-2-60.

4.2. Relation of Pressure Dependence to Physical Properties. Figure 3a compares the excess H₂ adsorption at 1 bar and 77 K with the computed isosteric heat Q_{st} evaluated at 1 bar for the five MOFs. We see a nearly linear relation with the effectiveness for H₂ density is in the order: IRMOF-2-96 > IRMOF-2-54 > IRMOF-2-60 > IRMOF-2-42 > IRMOF-2-24. At 30 bar we see that the order of excess H₂ adsorption is IRMOF-2-60 > IRMOF-2-96 > IRMOF-2-42 > IRMOF-2-54 > IRMOF-2-24.

Figure 3b shows the H₂ density at 30 bar and 77 K is linearly increased with free volume of MOFs.

Figure 3c shows how the excess H₂ adsorption depends on surface area, indicating the importance of surface area at 100 bar. Here the effectiveness has the order: IRMOF-2-60 > IRMOF-2-42 > IRMOF-2-96 > IRMOF-2-54 > IRMOF-2-24.

Here we calculate the surface area as the solvent accessible surface for rolling a ball of radius 1.2 Å around the system. For IRMOF-2-24 we calculate 4780 m²/g in excellent agreement with the experimental N₂ BET surface area (4746 m²/g),² indicating that we can ignore the effects of surfaces, grains, and defects in the experimental samples (similar results were also found for IRMOF-1 systems).¹²

This behavior is similar to previous results^{3d} for cubic crystalline MOFs, except that the previous study found that the total H₂ adsorption at intermediate pressure (e.g., 30 bar) correlates best with surface area.

We carried out a first-order linear regression analysis^{3d} to determine the contribution of each of these quantities to the total, as shown in Figure 3d. This analysis shows that

- at low pressure (1 bar) the excess amount adsorbed in Figure 3a–c is determined mainly by the heat of adsorption.
- At intermediate pressures (30 bar), the amount adsorbed is determined mostly by the free volume but also the surface area.
- At the highest pressure (100 bar) the amount adsorbed is determined mostly by the surface area but also the free volume.

In the case of total H₂ adsorption behavior, the order is similar to the excess case with the exception that the order at 100 bar is same to one at 30 bar, indicating that at 100 bar free volume of MOFs is the most important factor for H₂ storage.

These results show that a high free volume of the MOF is required to obtain the highest total uptake of H₂ while high surface area is required for the highest excess uptake of H₂. We find that the excess H₂ uptake of various MOFs at 90 bar depends linearly on the calculated surface area, which is consistent with recent experimental results from the Yaghi group.²

The linkers shown in Figure 1 can be classified into a single-linked aromatic ring group (IRMOF-2-24, IRMOF-2-42, and IRMOF-2-60) and a polyaromatic group (IRMOF-2-54 and IRMOF-2-96). In pure MOF cases, the polyaromatic group shows higher H₂ uptake at low pressure due to higher H₂ heat of adsorption (Figure 3a). Our previous MP2 calculation revealed that the more aromatic rings leads to the higher H₂ binding energy.⁴ For example, H₂ binding energies to benzene and naphthalene are −3.81 and −4.27 kJ/mol, respectively.⁴ However, a single-linked aromatic group has generally higher surface and free volume than a polyaromatic group. Exposing the latent edges of the six-membered rings lead to significant enhancement of specific surface area.^{1c} A surface area of the IRMOF-2-42 is 5722 m²/g, which is higher than 5112 m²/g for the IRMOF-2-54 and 5175 m²/g for the IRMOF-2-96 although the IRMOF-2-42 is consisted of aromatic linkers with lower numbers of carbon atoms. Thus at high pressure a single-linked aromatic group can store more H₂ than a polyaromatic group.

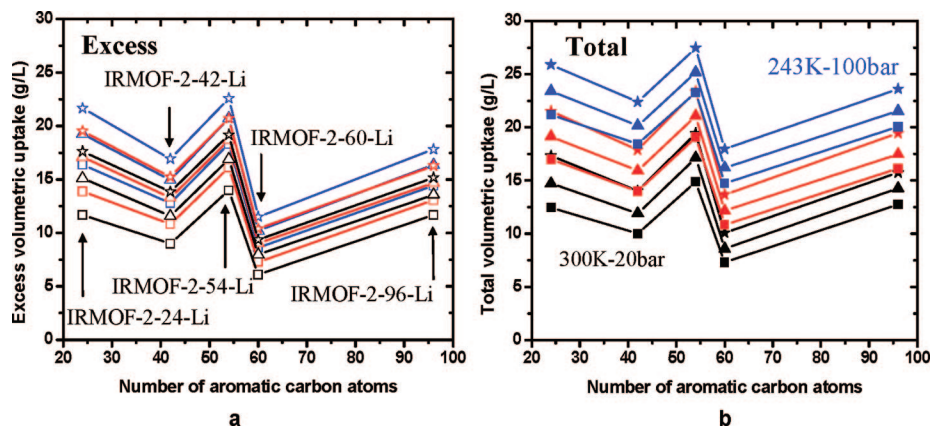


Figure 6. Predicted excess (a) and total (b) H₂ density in volumetric units for IRMOF-Li as a function of temperature and pressure. Here the symbol code is 243 K = star, 273 K = triangle, 300 K = square and black = 20 bar, red = 50 bar, and blue = 100 bar.

5. Results and Discussion for New Li-Doped Hexagonal MOF Materials

As seen in Figure 4a, the calculated H₂ storage amount of pure MOFs at 300 K is very low. The highest H₂ uptake is 1.2 wt % at 100 bar for IRMOF-2-96, which remains much lower than the 2010 DOE target.

Previously we had considered doping Li into cubic crystalline, MOFs where our GCMC simulations found the significant increase of H₂ storage at 300 K.⁶ This results from the strong stabilization of molecular H₂ by Li bonded to the aromatics. For example, Li-doped IRMOF-1-30-Li (previously denoted MOF-C30) with a Li concentration of C₃Li has 5.2 wt % at 300 K and 100 bar.⁶

Thus to improve H₂ density of hexagonal MOFs at ambient temperature, we investigated the effect of Li doping on H₂ storage capacity of hexagonal MOFs. Indeed Figure 4 shows that Li doping improves remarkably the H₂ uptake at 300 K. We find that Li doping leads to 'type I' H₂ isotherm curves¹³ rather than the linear isotherms in pure MOFs. We also find that the isotherms are not saturated up to 100 bar. At 300 K the best Li-doped MOF is IRMOF-2-96-Li, which stores 4.4 wt % at 20 bar, 5.0 wt % at 50 bar, and 5.6 wt % at 100 bar. For cubic crystalline Li-doped IRMOF-1-30 we found 3.9 wt % at 20 bar and 4.6 wt % at 50 bar.⁶

We also predicted the H₂ storage capacity for Li-doped MOFs at various temperature and pressure conditions (Figure 4b). For all temperatures and pressures, we find that IRMOF-2-96-Li has the highest gravimetric H₂ density. For example, at a pressure of 100 bar, IRMOF-2-96-Li has 5.6 (300 K), 6.0 (273 K), and 6.5 wt % (243 K). Thus IRMOF-2-96-Li reaches the DOE target of 6.0 wt % up to 273 K. At 50 bar IRMOF-2-96-Li can store 6.0 wt % H₂ at 243 K, a pressure much lower than the (100 bar) required for IRMOF-1-30-Li.⁶ In addition, at 243 K and 100 bar, both IRMOF-2-54-Li and IRMOF-2-60-Li meet the DOE target. At 273 K, only IRMOF-2-96-Li reaches the DOE target at 100 bar.

Experimentally pure MOFs show reversible adsorption and desorption behavior for hydrogen.¹ Moreover, experiments by Mulfort and Hupp show that there is no hysteresis between adsorption and desorption isotherms of H₂ in the Li-doped MOFs synthesized using redox-active ligands,¹⁴ supporting our result that H₂ binding of Li-doped MOFs shown in Figure 4 is reversible. Indeed Mulfort and Hupp confirm our prediction that Li doping enhances H₂ storage capacity.

Figure 4 shows that the order of excess gravimetric H₂ density of Li doped MOFs at 300 K is IRMOF-2-96-Li > IRMOF-2-

54-Li > IRMOF-2-60-Li > IRMOF-2-42-Li > IRMOF-2-24-Li up to a pressure of 100 bar.

This order of binding does not correlate individually with isosteric heat of adsorption, free volume, or surface area. However, we do find a linear correspondence of the H₂ density with a combination of heat of adsorption and surface area (see Figure 5). Thus for Li-doped MOFs, the H₂ adsorption behavior at 300 K depends on both heat of adsorption and surface area up to 100 bar.

In the Li-doped MOFs, the H₂ uptake relies on both heat of adsorption and surface area in all pressure range (Figure 5). A single-linked aromatic ring group occupies the only C₆Li composition irrespective of the number of carbon atoms, while in a polyatomic group the more carbon atoms can show the higher lithium concentration, leading to significant increase of heat of adsorption of H₂ due to strong interaction between H₂ and Li. Therefore although a surface area of IRMOF-2-96-Li is lower than those of IRMOF-2-60-Li and IRMOF-2-42-Li, it can store most H₂ among MOFs considered in this work.

For a hydrogen storage medium to be practical, one must consider both volumetric uptake and gravimetric uptake. Thus, we calculated excess and total volumetric H₂ density for Li-doped MOFs as functions of temperature and pressure, which is shown in Figure 6. The best volumetric H₂ storage at all temperatures and pressures is found for the IRMOF-2-54-Li system. At 100 bar, it leads to excess adsorption H₂ of 19.2 (300 K), 20.7 (273 K), and 22.6 g/L (243 K), which is lower than the 2010 DOE target (45.0 g/L).

Considering total H₂ adsorption, the IRMOF-2-54-Li shows H₂ uptake amount of 23.3 (300 K), 25.2 (273 K), and 27.5 g/L (243 K) at 100 bar. Although IRMOF-2-54-Li has lower Li concentration than IRMOF-2-96-Li, the volumetric uptake is higher in IRMOF-2-54-Li because of its lower free volume. This effect is obviously observed in a single-linked aromatic group. In the MOFs, the Li concentration is fixed by C₆Li, however free volume is increased with the number of carbon atoms, leading to the fact that in volumetric H₂ uptake aspect IRMOF-2-60-Li is worst due to the highest free volume size.

Finally, we compare hexagonal and cubic MOFs as hydrogen storage media. Here we use same methods as reported previously⁴ for H₂ adsorption behavior of cubic MOF with polyaromatic linkers and Zn₄O(CO₂)₆ metallic connectors. Our simulations predicted that the IRMOF-1-30 system is the best candidate among cubic MOFs with a maximum H₂ storage capacity of 7.2 wt % at 77 K.⁴ This is lower than all the hexagonal MOFs considered in this present work, where we

find 7.5 wt % for IRMOF-2-24, 8.9 wt % for IRMOF-2-42, 8.4 wt % for IRMOF-2-54, 9.7 wt % for IRMOF-2-60, and 8.7 wt % for IRMOF-2-96). Since the cubic and hexagonal MOFs have similar chemical architectures, the adsorption energies for H₂ in the two families are similar. The difference in the maximum H₂ storage capacity is related to the surface areas of the MOFs as explained in Figure 3. Cubic IRMOF-1-30 has 30 carbon atoms in aromatic rings, 6 more than the hexagonal IRMOF-2-24. However, the surface area of MOF-C30 (4641 m²/g) is lower than that of IRMOF-2-24 (4780 m²/g), leading to increased H₂ storage for the hexagonal MOF. Therefore, we consider that the triconnecting linkers of the hexagonal MOF are responsible for the higher surface area of the MOF compared to the biconnecting linkers of the cubic MOFs.

In Li-doped MOFs, IRMOF-1-30-Li with a C₅Li concentration stores 5.2 wt % H₂ at 300 K and 100 bar,⁶ which is lower than the 5.6 wt % of IRMOF-2-96-Li which a C_{5.05}Li concentration, but it is higher than other hexagonal MOFs (3.8 wt % for IRMOF-2-24-Li, 4.0 wt % for IRMOF-2-42-Li, 5.0 wt % for IRMOF-2-60-Li, and 5.1 wt % for IRMOF-2-54-Li).

Figure 5 clarifies the H₂ adsorption behavior for Li-doped MOFs near room temperature, showing that it depends on both heat of adsorption and surface area. Therefore although the lithium concentration (C_{5.05}Li) in IRMOF-2-96-Li is similar to that (C₅Li) in IRMOF-1-30-Li (they have similar H₂ binding energies), the former shows higher H₂ uptake than the latter since the surface area (5278 m²/g) of IRMOF-2-96-Li is higher than that (4693 m²/g) of IRMOF-1-30-Li. As a result Li-MOF-C30 can barely reach the 2010 DOE target at 243 K and 100 bar, but IRMOF-2-96-Li meets the target even at 50 bar and 243 K. Indeed IRMOF-2-96-Li successfully reaches the target at 273 K. These results indicate that it is the higher surface area that makes hexagonal MOF superior to cubic MOF.

6. Summary

Summarizing, we used GCMC simulations to show that IRMOF-2-60 can achieve 9.7 wt % H₂ storage at 77 K and 90 bar pressure, better than any other material for associative binding of H₂ at this temperature. This excess H₂ uptake at 77 K for hexagonal MOFs is mainly determined by the heat of adsorption of H₂ at low pressure (1 bar), by the free volume of MOFs at intermediate pressure (30 bar), and by the surface area at high pressure (100 bar).

We find that Li doping into the MOFs leads to significant enhancement of H₂ uptake at ambient temperature. Indeed IRMOF-2-96-Li leads to 6.5 wt % reversible H₂ storage at 243 K and 100 bar, reaching the 2010 DOE target. For Li-doped MOFs the H₂ uptake behavior near room temperature both the heat of adsorption and the surface area are important. Thus since hexagonal MOFs generally have higher surface area than cubic ones, they lead to higher H₂ uptake under the same conditions.

The accuracy of these GCMC simulations (using FFs determined from accurate QM calculations) was validated by

comparison with the experimental loading for IRMOF-2-24 up to a pressure of 100 bar.

Acknowledgment. We thank Prof. Omar M. Yaghi (UCLA) for many helpful discussions. We thank DOE (DE-FG01-04ER04-20) for partial support. The facilities of the Materials and Process Simulation Center were supported by ONR-DURIP and ARO-DURIP. Additional support of the MSC was provided by MURI-ARO, MURI-ONR, DOE (ASC, FETL), NSF (NIRT), NIH, Boehringer-Ingelheim, Chevron, Dow-Corning, Intel, Pfizer, and Allozyne.

References and Notes

- (1) (a) Eddaoudi, M.; Kim, J.; Rosi, N.; Vodak, D. T.; Wachter, J.; O'Keeffe, M.; Yaghi, O. M. *Science* **2002**, *295*, 469. (b) Rosi, N. L.; Eckert, J.; Eddaoudi, M.; Vodak, D. T.; Kim, J.; O'Keeffe, M.; Yaghi, O. M. *Science* **2003**, *300*, 1127. (c) Chae, H. K.; Siberio-Perez, D. Y.; Kim, J.; Go, Y.-B.; Eddaoudi, M.; Matzger, A. J.; O'Keeffe, M.; Yaghi, O. M. *Nature* **2004**, *427*, 523. (d) Zhao, X.; Xiao, B.; Fletcher, A. J.; Thomas, K. M.; Nradshaw, D.; Roesseinsky, M. J. *Science* **2004**, *306*, 1012. (e) Rosi, N. L.; Millward, A. R.; Park, K. S.; Yaghi, O. M. *J. Am. Chem. Soc.* **2004**, *126*, 5666. (f) Lee, E. Y.; Suh, M. P. *Angew. Chem., Int. Ed.* **2004**, *43*, 2798. (g) Keyes, S. S.; Long, J. R. *J. Am. Chem. Soc.* **2005**, *127*, 6506. (h) Rowsell, J. L. C.; Yaghi, O. M. *Angew. Chem., Int. Ed.* **2005**, *44*, 4670. (i) Kesani, B.; Cui, Y.; Smith, M. R.; Bitter, E. W.; Bockrath, B. C.; Lin, W. *Angew. Chem., Int. Ed.* **2005**, *44*, 72. (j) Panella, B.; Hirsher, M.; Pütter, H.; Müller, U. *Adv. Func. Mater.* **2006**, *16*, 520. (k) Lin, X.; Jia, J.; Zhao, X.; Thomas, K. M.; Blake, A. J.; Walker, G. S.; Chamness, N. R.; Hubberstey, P.; Schröder, M. *Angew. Chem., Int. Ed.* **2006**, *45*, 7358. (l) Sun, D.; Ma, S.; Ke, Y.; Collins, D. J.; Zhou, H. *J. Am. Chem. Soc.* **2006**, *128*, 3896. (m) Dincă, M.; Han, W. S.; Liu, Y.; Dailly, A.; Brown, C. M.; Long, J. R. *Angew. Chem., Int. Ed.* **2007**, *46*, 1419. (n) Furukawa, H.; Miller, M. A.; Yaghi, O. M. *J. Mater. Chem.* **2007**, *17*, 3197.
- (2) Wong-Foy, A. G.; Matzger, A. J.; Yaghi, O. M. *J. Am. Chem. Soc.* **2006**, *128*, 3494.
- (3) (a) Sagara, T.; Ortony, J.; Ganz, E. *J. Chem. Phys.* **2005**, *123*, 214707. (b) Yang, Q.; Zhang, C. *J. Phys. Chem. B* **2005**, *109*, 11862. (c) Dailly, A.; Vajo, J. J.; Ahn, C. C. *J. Phys. Chem. B* **2006**, *110*, 1099. (d) Frost, H.; Düren, T.; Snurr, R. Q. *J. Phys. Chem. B* **2006**, *110*, 9565.
- (4) Han, S. S.; Deng, W.-Q.; Goddard, W. A. *Angew. Chem., Int. Ed.* **2007**, *46*, 6289.
- (5) <http://www.eere.energy.gov/hydrogenandfuels/mypp/>.
- (6) Han, S. S.; Goddard, W. A. *J. Am. Chem. Soc.* **2007**, *129*, 8422.
- (7) Jaguar 6.5, Schrödinger, Inc., Portland, OR, 1991–2000. Xu, X.; Goddard, W. A. *Proc. Natl. Acad. Sci. U.S.A.*, **2004**, *101*, 2673.
- (8) Mayo, S. L.; Olafson, B. D.; Goddard, W. A. *J. Phys. Chem.* **1990**, *94*, 8897.
- (9) The GCMC calculations were carried out using the sorption module of Cerius 2 (Accelrys, San Diego) with the FF described in SI.
- (10) (a) Garberoglio, G.; Skoulidas, A. I.; Johnson, J. K. *J. Phys. Chem. B* **2005**, *109*, 13094. (b) Zhou, W.; Hui, W.; Hartman, M. R.; Yildirim, T. *J. Phys. Chem. C* **2007**, *111*, 16131.
- (11) In calculating the Q_{st} , we employ the fluctuation formula, $Q_{st} = k_B T - \{ \langle NU \rangle - \langle N \rangle \langle U \rangle \} / \{ \langle N^2 \rangle - \langle N \rangle \langle N \rangle \}$ where N and U are the number of H₂ and the total internal energy in any given configuration respectively, and $\langle \rangle$ represents a configuration average. Nicholson, D.; Parsonage, N. G. *Computer Simulation and the Statistical Mechanics of Adsorption*, Academic Press; London, 1982.
- (12) (a) Walton, K. S.; Snurr, R. Q. *J. Am. Chem. Soc.* **2007**, *129*, 8552. (b) Düren, T.; Millange, F.; Férey, G.; Walton, K. S.; Snurr, R. Q. *J. Phys. Chem. C* **2007**, *111*, 15350.
- (13) Fletcher, A. J.; Thomas, K. M.; Rosseinsky, M. J. *J. Solid State Chem.* **2005**, *178*, 2491.
- (14) Mulfort, K. L.; Hupp, J. T. *J. Am. Chem. Soc.* **2007**, *129*, 9604.

JP800832B